Journal of Solid State Chemistry **168,** 675–689 (2002)
doi:10.1006/jssc.2002.9766

Why do Physicists Love Charge-Transfer Salts?

John Singleton[1]

Department of Physics, University of Oxford, The Clarendon Laboratory, Parks Road, Oxford OX1 3PU, United Kingdom

Received February 27, 2002; in revised form April 1, 2002; accepted April 3, 2002

I describe some of the phenomena encountered in charge-transfer salts that make them very attractive for condensed-matter physicists. These materials exhibit many interesting electronic properties, including reduced dimensionality, strong electron–electron and electron–phonon interactions and the proximity of antiferromagnetism, insulator states and superconductivity. A wide variety of low-temperature groundstates have been observed in the salts; frequently, one is able to move between these states by applying magnetic field, temperature, pressure or "chemical pressure". In spite of this complex behavior, the charge-transfer salts possess very simple electronic bandstructure which it is often possible to measure in great detail. Hence, one can use the salts as "model systems" in which tractable theoretical calculations for phenomena such as superconductivity are compared directly with experiment.

1. INTRODUCTION

For most of the 20th century, solid-state physicists chiefly studied *inorganic* elements, alloys, and simple compounds. Their assumption was that fundamental physics research is most usefully concentrated on *chemically simple* materials. However, in recent years, there has been a growing interest in the physics community in charge-transfer salts made up from small organic molecules (1). Although to a physicist, these systems can look chemically complex, their electronic properties are often beautifully simple (1–3). As a result, charge-transfer salts can often provide a great deal of information about very basic phenomena like electronic band formation (4), superconductivity (5) and magnetism (6).

In this brief article, I hope to convey some of the exciting physics which is being accomplished using charge-transfer salts. A recurring theme will be the similarity of charge-transfer salts to other fundamentally interesting systems; for example, they share many properties with the famous "high-T_c" cuprate superconductors (7)—a layered structure, a close relationship between superconductivity and antiferromagnetism, strong electron–electron and electron–phonon interactions and an exotic type of superconductivity known as "*d*-wave" (5). However, in contrast to the cuprates, the charge-transfer salts are very clean systems, permitting many detailed measurements of the electronic properties which have not been possible in the high T_c's (5). The charge-transfer salts therefore emerge with a considerable advantage as "model systems" for research into exotic superconductivity; many of their underlying electronic properties can be measured to great precision. A number of recent theoretical studies of superconductivity have begun to exploit this (8,9).

2. CHARGE-TRANSFER SALTS AND THE PHYSICS OF BAND FORMATION

Charge-transfer salts are formed when a number j of donor molecules D jointly donate an electron to a second type of molecule (or collection of molecules) which we label X, to form the compound D_jX (2); owing to its charge, X is usually referred to as the anion molecule. The charge-transfer fulfills two functions; it serves to bind the charge-transfer salt together and also acts as a "dopant" (acceptor) by leaving behind a hole (an empty electron state), jointly shared between the j donor molecules (1).

A typical donor molecule is bis(ethylenedithio)tetrathiofulvalene (see Scheme). Physicists tend to regard such molecules as simple units or "building blocks" which can

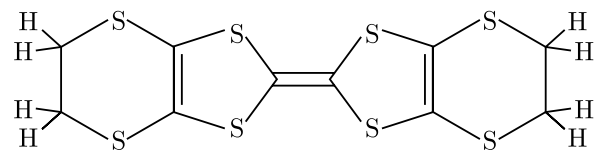

SCHEME 1. The bis(ethylenedithio)tetrathiofulvalene (BEDT-TTF) molecule, a typical "building block" for making charge-transfer salts.

[1]To whom correspondence should be addressed. E-mail: j.singleton1@physics.oxford.ac.uk. Current address: National High Magnetic Field Laboratory (MST-NHMFL), TA-35, MS-E536, Los Alamos National Laboratory, LosAlamos, New Mexico 87545.

0022-4596/02 $35.00

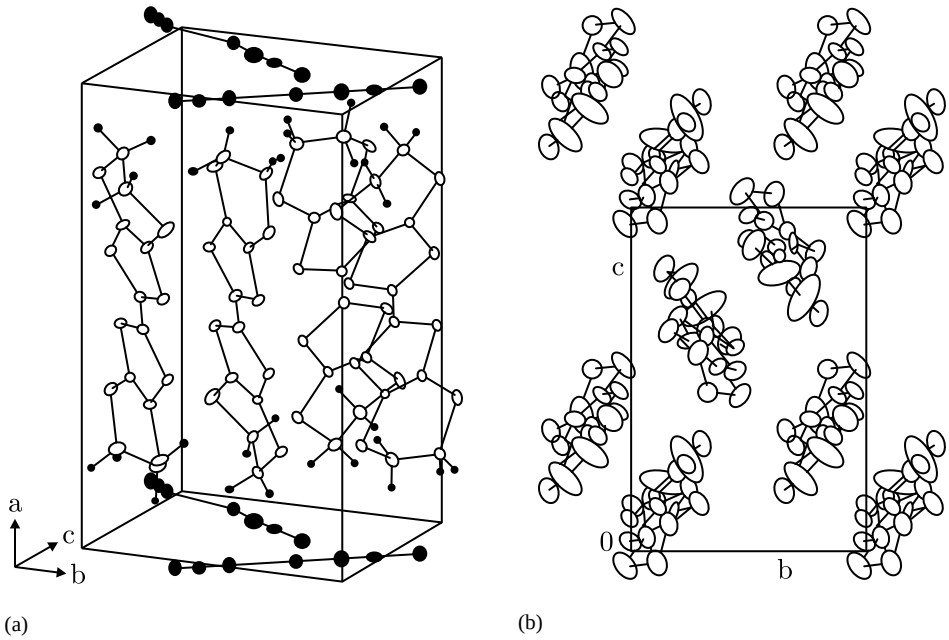

FIG. 1. Structure of the BEDT-TTF superconductor κ-(BEDT-TTF)$_2$Cu(NCS)$_2$ (after Ref. (11)). (a) Side view of molecular arrangement; the BEDT-TTF molecules packed in planes separated by layers of the smaller Cu(NCS)$_2$ anions. (b) View downwards onto the BEDT-TTF planes, showing that the BEDT-TTF molecules are packed in closely spaced pairs(*dimers*), allowing substantial overlap of the molecular orbitals. The unit cell edges are 16.248, 8.44 and 13.124 Å at room temperature (11).

be used to make up the electronic bands of electrically conducting solids; the electronic bands are based on the donor molecule's molecular orbitals (1,3,4). In a charge-transfer salt, the donor molecules are stacked next to each other so that the molecular orbitals overlap; crudely one might say that this enables electrical conductivity as the electrons can then jump from molecule to molecule. The readiness with which this transfer of an electron from one donor molecule to another is parameterized by an energy known as the *transfer integral* (10).

Figure 1 shows the molecular arrangements in the BEDT-TTF charge-transfer salt κ-(BEDT-TTF)$_2$ Cu(NCS)$_2$, a $T_c \sim 10.4$ K superconductor (11). (Here the κ denotes the packing arrangement of the BEDT-TTF molecules.) The BEDT-TTF molecules are packed into layers, separated by planes of the Cu(NCS)$_2$ anion molecules. Within the BEDT-TTF layers, pairs of molecules *dimers* are in close proximity to each other, so that hopping of electrons or holes from molecule to molecule can occur with relative ease; in these directions, the transfer integrals are relatively large, typical values ranging from 10 s of meV to $\sim$100 meV (see Ref. (12) and references therein). Conversely, in the direction perpendicular to the BEDT-TTF planes, the BEDT-TTF molecules are well separated from each other; the transfer integral(s) will be very small; values from $\sim$0.04 to $\sim$0.2 meV have been inferred from experiments (12,13).

In simple terms, we therefore have layers of "conductor" (the BEDT-TTF molecules) separated from each other by layers of "packing" (the Cu(NCS)$_2$ molecules) which do not contribute to the electrical conductivity. As a result of this structure, the electronic properties of charge-transfer salts can for many purposes be regarded as two dimensional or quasitwo dimensional (12).

Charge-transfer salts are attractive to physicists because they are very versatile systems for studying the electronic bandstructure that allows electrical conduction (3). First of all, one can change the anion molecule for a shorter or longer one; in the former case this pushes the BEDT-TTF molecules close together, in the latter it pulls the BEDT-TTF molecules further apart (1). Pushing the BEDT-TTF molecules closer together will tend to give larger transfer integrals and therefore wider electronic energy bands and a higher electrical conductivity (10). On the other hand, pulling the molecules further apart may eventually make the transfer integrals sufficiently small to generate an insulator (a so-called Mott insulator) (2,6). Using the example shown in Fig. 1, κ-(BEDT-TTF)$_2X$ can be made with a variety of other anion molecules, including $X =$ Cu[N(CN)$_2$]Br (longer than Cu(NCS)$_2$), Cu[N(CN)$_2$]Cl (even longer), and I_3 (shorter than Cu(NCS)$_2$) (1). For $X =$ Cu[N(CN)$_2$]Cl, one obtains an insulator (6). The use of different anions to vary the unit cell size is often referred to as "chemical pressure" (2); it nicely complements the application of actual hydrostatic pressure. The application of both kinds of pressure can allow a wide range of behavior to be accessed in one family of charge-transfer salts (see, e.g., Ref. (3,6) and references therein).

By using more drastic changes of anion, or different growth conditions, one can make the BEDT-TTF molecules pack in different arrangements (1). As the BEDT-TTF molecules are long and flat (unlike single atoms), the resulting electronic properties will depend strongly on the way in which the BEDT-TTF molecules are arranged with respect to each other; one can, for example, make materials with very anisotropic intralayer conductivity (2). It is therefore convenient to classify charge-transfer salts according to their crystal structures, as each packing arrangement results in a distinct class of electronic energy bands (1,3). The main arrangements are labelled the α, β, β'', δ, χ, κ, θ and λ phases (1).

Finally, one can change the molecular building blocks themselves; for example, when the innermost four sulfur atoms of BEDT-TTF are replaced by selenium, one obtains BETS (bis(ethylenedithio)tetraselenafulvalene), which can also be used to produce charge-transfer salts such as λ-$(BETS)_2GaCl_4$ (13) and the recent field-induced superconductor λ-$(BETS)_2FeCl_4$ (14). There are many other varieties of a similar nature, with acronyms such as BEDO and MDT-TTF (1).

3. QUASIPARTICLES AND INTERACTIONS

A simple bandstructure calculation essentially uses ions and molecules which are rigidly fixed in a perfectly periodic arrangement to obtain a periodic potential and hence the bands (10). However, the ions and/or molecules in a substance will in general be charged, or at the very least possess a dipole moment; as an electron or hole passes through the solid, it will tend to distort the lattice around it owing to the Coulomb interactions between the ions and molecules and its own charge (5,10,17). This leads to the electron or hole being accompanied by a strain field as it moves through the substance; alternatively one can consider the electron or hole being surrounded by virtual phonons, leading to a change in self energy (5,10). Similarly, self-energy effects due to the interactions between the conduction electrons themselves must be taken into account (5,10,17).

The inclusion of such effects leads to the idea of "quasiparticles", excitations of an interacting electron system which obey Fermi–Dirac statistics and which "look like" conduction electrons or holes in many ways, but which possess renormalized effective masses and scattering

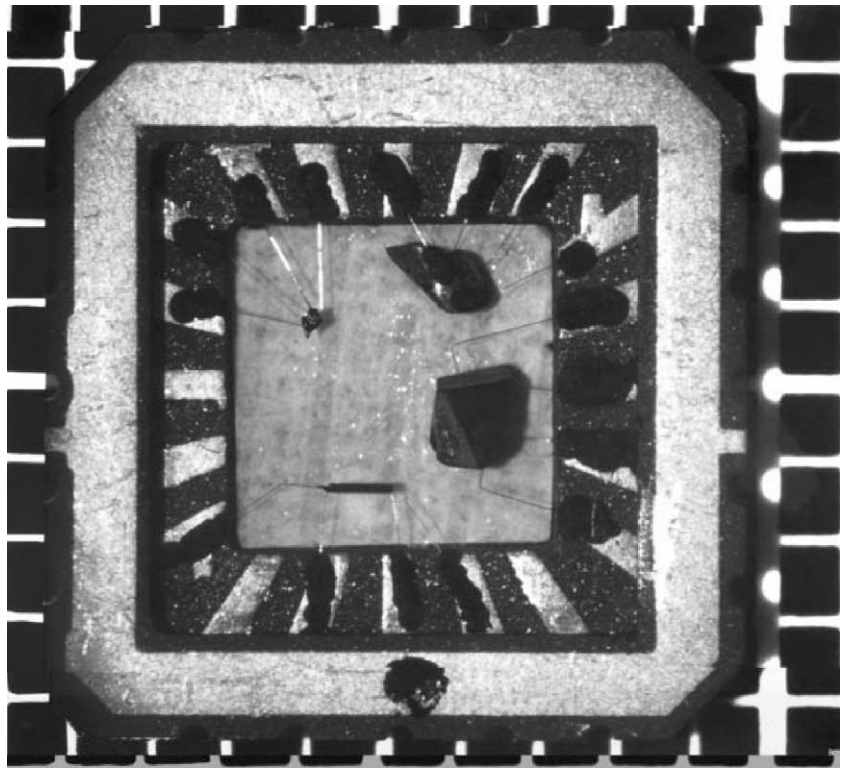

FIG. 2. Single crystals of charge-transfer salts mounted for magneto-transport experiments. The crystals are usually grown using electrocrystallization (1,2); they are of exceptionally high quality, but their size is limited; the squares on the backing material are 1×1 mm^2. Electrical connections to the samples are made using 12 μm platinum wire attached with graphite-bearing paint applied using a single human hair as a brush. Recent efforts in Russia (15) have made much larger samples as surface films on a polymer substrate. Although such structures do combine superconductivity with useful mechanical properties such as flexibility, their crystal quality is still far below that of the single crystals (16).

rates (10, 17). (The effective mass parameterizes the way in which a quasiparticle can respond to an external force. The effective mass also gives a measure of the density of quasiparticle states at the Fermi energy. See, e.g., Ref. (10).) A collection of interacting electrons which can be treated (using Fermi–Dirac statistics) as a collection of quasiparticles is often known as a *Fermi liquid*; by contrast, a collection of non-interacting electrons is called a *Fermi gas* (10).

Such considerations seem to be very important in charge-transfer salts (5,18). A number of different experimental techniques have been employed to show that the experimental effective masses of quasiparticles in charge-transfer salts can be a factor ~ 5 larger than those predicted in bandstructure calculations (see Section 2.4 of Ref. (5) for a summary). I have in the past (3) suggested some similarities between the charge-transfer salts and semiconductor heterostructures and superlattices. However, the charge-transfer salts contain areal electron and hole densities per layer which are some two orders of magnitude higher than those achievable in semiconductor two-dimensional layers; as a consequence, the electron–electron and electron–phonon interactions are no longer the small perturbations that they are in the semiconductor systems but act as major influences in determining the groundstate observed (18); hence, the organics are a very useful system for the study of many-body effects such as electron–electron and electron–phonon interactions. As we shall see in the next section, the simplicity of the electronic bands is of considerable assistance in such work (5,8,9,18).

4. FERMI SURFACES

From the point of view of a physicist, the defining property of a metal is that it possesses a *Fermi surface*, that is, a constant-energy surface in k-space which separates the filled quasiparticle states from empty states at absolute zero ($T = 0$) (10). The energy of a quasiparticle at the Fermi surface is known as the *Fermi energy*, E_F (10). The shape of the Fermi surface is determined by the dispersion relationships (energy versus $\mathbf{k}$ relationships) $E = E(\mathbf{k})$ of each partially filled band and the number of electrons (or holes) to be accommodated. Virtually all of the properties of a metal are determined by the quasiparticles at the Fermi surface, as they occupy states which are adjacent in energy to empty states; therefore they are able to respond to external forces and other perturbations (10).

As has been mentioned above, charge-transfer salts are highly anisotropic; most of the quasiparticle motion occurs within the highly conducting planes (2,4,12). The Fermi-surface topology is dominated by this consideration; the interlayer motion is far less important (12). In this section we shall therefore examine the cross-sections of the Fermi surfaces parallel to the highly conducting planes.

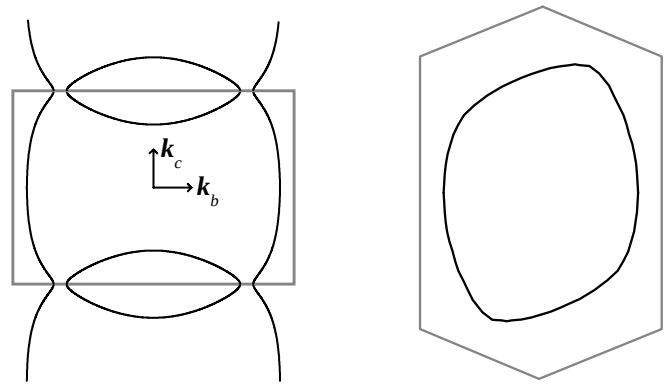

FIG. 3. (a) Brillouin zone and Fermi-surface of κ-(BEDT-TTF)$_2$Cu(NCS)$_2$, showing the open, quasione-dimensional sections, and the closed, quasitwo-dimensional pocket (12). (b) Brillouin zone and Fermi-surface of β-(BEDT-TTF)$_2$IBr$_2$ (18).

Figure 3(a) shows a section through the first Brillouin zone and Fermi surface of κ-(BEDT-TTF)$_2$Cu(NCS)$_2$ (based on parameters given in Ref. (12)).

The Fermi surface may be understood by examining Fig. 1(b). Note that the BEDT-TTF molecules are packed in pairs called *dimers*; if we consider each dimer as a unit, it will be seen that it is surrounded by four other dimers. We thus expect the bandstructure to be fairly isotropic in the plane, because there will be substantial, similar transfer integrals in these directions (8). The unit cell contains two dimers, each of which contributes a hole (in the charge-transfer process, two BEDT-TTF molecules jointly donate one electron to the anion) (12). Thus, to a first approximation, the Fermi surface for holes might be expected to be roughly circular with the same area as the Brillouin zone as there are two holes per unit cell. (The Brillouin-zone is the primitive unit cell of the reciprocal (k-space) lattice. The k-space size of the Fermi surface follows from the properties of phase space. Each quasiparticle donated by a unit cell contributes a volume to the Fermi surface equivalent to half the volume of the Brillouin zone. See, e.g., Ref. (10).) As can be seen from Fig. 3(a), the Fermi surface is *roughly* like this; however, the Fermi surface intersects the Brillouin zone boundaries in the **c** direction, so that band gaps open up (10). The Fermi surface thus splits into open (electron-like) sections (often known as *Fermi sheets*) running down two of the Brillouin-zone edges and a closed hole pocket (referred to as the "α pocket" (1,2)) straddling the other; it is customary to label such sections "quasione dimensional" and "quasitwo dimensional" respectively. The names arise because the group velocity $\mathbf{v}$ of the electrons is given by (10)

$$\hbar\mathbf{v} = \nabla_{\mathbf{k}} E(\mathbf{k}). \qquad [1]$$

The Fermi surface is a surface of constant energy; Eq. [1] shows that the velocities of electrons at the Fermi surface

will be directed perpendicular to it. Therefore, referring to Fig. 3, electrons on the closed Fermi-surface pocket can possess velocities which point in any direction in the (k_b, k_c) plane; they have freedom of movement in two dimensions and are said to be *quasitwo dimensional*. By contrast, electrons on the open sections have velocities predominantly directed parallel to k_b and are *quasione dimensional*.

Figure 3(b) shows the Fermi-surface topology and Brillouin zone of β-(BEDT-TTF)$_2$IBr$_2$ (19). In this case, there is one hole per unit cell (1,5), so that the Fermi-surface cross-sectional area is half that of the Brillouin zone; only a quasitwo-dimensional pocket is present.

From a physicist's point of view, the simplicity of the Fermi surfaces of charge-transfer salts is attractive. Often, they are remarkably similar to "model" or "toy" Fermi surfaces used to explain fundamental effects such as magnetic breakdown (see below) (20–22). Moreover, as has been mentioned in the previous section, many-body effects such as electron–electron and electron–phonon interactions are very significant in the charge-transfer salts. Many-body effects are also very important in materials such as the *heavy-fermion compounds* (23); however, the organics have much simpler Fermi surfaces and experimental conditions required for their study are often much less difficult (3).

5. FERMI SURFACE MEASUREMENTS

Some 15 years ago, it was realized that charge-transfer salts are usually very "clean" systems from an electronic point of view (2,4,3,17). Typical hole mean-free paths of thousands of Ångstroms at low temperatures are not unknown. It was therefore apparent that the high-magnetic field techniques that had been used to discover the Fermi surfaces of very pure single crystals of metallic elements (10,24) could be applied to the organics. Pioneers in this field included Oshima and colleagues at Tokyo (25), Pratt and Hayes at Oxford (26) and Kang *et al.* (27) in Paris. A thoughtful review of the early work was given by another pioneer, Naoki Toyota, and his colleagues (17); more recent work is summarized in Ref. (3).

In a magnetic field, the motion of quasiparticles becomes partially quantized according to the equation (3,10)

$$E(\mathbf{B}, k_z l) = \frac{\hbar e|\mathbf{B}|}{m^*}\left(l + \frac{1}{2}\right) + E(k_z). \qquad [2]$$

Here $E(k_z)$ is the energy of the (unmodified) motion parallel to $\mathbf{B}$, l is a quantum number $(0, 1, 2, \ldots)$ and m^* is an orbitally averaged effective mass. The magnetic field quantises the motion of the quasiparticles in the plane perpendicular to $\mathbf{B}$; the resulting levels are known as *Landau levels*, and the phenomenon is called *Landau quantization*. The Landau-level energy separation is given by $\hbar$ multiplied by the angular frequency $\omega_c = e\mathbf{B}/m^*$; this is known as the *cyclotron frequency* because it corresponds to the semiclassical frequency at which the quasiparticles orbit the Fermi surface (3,10).

Magnetic quantum oscillations (3,4,24) are caused by the Landau levels passing through the Fermi energy. (Strictly it is the *chemical potential* μ, rather than the Fermi energy, which is important here. However $\mu \equiv E_F$ at $T = 0$, and $\mu \approx E_F$ for virtually all experimental temperatures of interest (10)). This results in an oscillation of the electronic properties of the system, periodic in $1/|\mathbf{B}|$. From an experimental standpoint, the oscillations are usually measured in the magnetization (de Haas–van Alphen effect) or the resistivity (Shubnikov–de Haas effect) (3,4,24).

Landau quantization only occurs for sections of Fermi surface corresponding to semiclassical *closed* k-space orbits in the plane perpendicular to $\mathbf{B}$; the frequency of the oscillation (in Tesla) is given by $F = (\hbar/2\,\pi e)A$, where A is the cross-sectional k-space area of the orbit (3,4,24). An example is given in Fig. 4, which shows Shubnikov–de Haas oscillations in the magnetoresistance of κ-(BEDT-TTF)$_2$Cu(NCS)$_2$ (the field was applied perpendicular to the quasitwo-dimensional planes). Turning first to Fig. 4(a), a single frequency of oscillations is observed, caused by the quasitwo-dimensional α pocket of the Fermi surface. The frequency (600 ± 3 T in this case) allows one to deduce the cross-sectional area of the α pocket (3,4). On increasing the temperature, the oscillations decrease in amplitude, owing to the thermal smearing of the Fermi–Dirac distribution function (3,10,24). The temperature dependence of the oscillation amplitude can be used to derive the orbitally averaged effective mass of the quasiparticles orbiting the α pocket (3,4) (3.5 ± 0.1 m_e in this case (3)). Finally, the oscillations increase in amplitude with increasing magnetic field; this field dependence allows one to derive the scattering time τ (3) (3 ps for the data shown (5)).

At higher magnetic fields (Fig. 4(b)), an additional set of higher frequency oscillations becomes observable. These are due to a phenomenon known as *magnetic breakdown* (3,20–22); the cyclotron energy of the quasiparticles becomes high enough for them to tunnel (in k-space) across the gaps between the quasitwo-dimensional pocket and the quasione-dimensional sheets, so that a semiclassical orbit around the whole Fermi surface (a so-called β orbit) can be completed (3,21). The large cross-sectional area of this orbit gives rise to a higher Shubnikov–de Haas oscillation frequency.

Figure 5 shows a second technique, known as *angle-dependent magnetoresistance oscillations* (AMROs), largely pioneered by Mark Kartsovnik and colleagues in Chernogolovka (19). In this case, the technique has been applied to the superconductor β''-(BEDT-TTF)$_2$SF$_5$CH$_2$CF$_2$SO$_3$

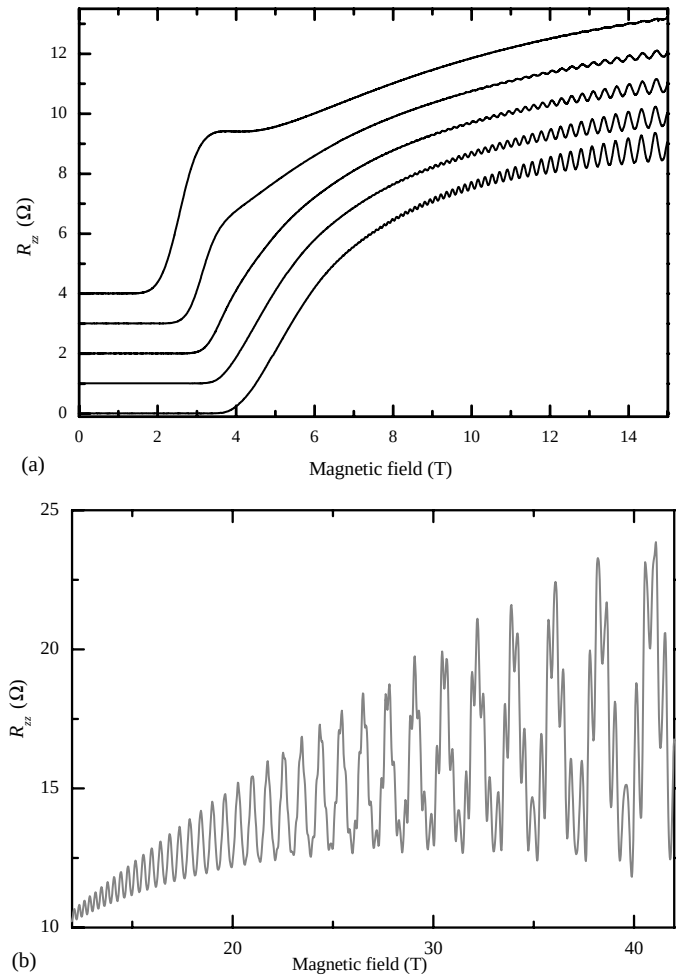

FIG. 4. Magnetoresistance measurements of the organic superconductor κ-(BEDT-TTF)$_2$Cu(NCS)$_2$ (magnetic field applied perpendicular to the quasitwo-dimensional planes). (a) Low-field measurements, showing the superconducting to normal transition and, at higher fields, Shubnikov–de Haas oscillations caused by the quasitwo-dimensional α pocket of the Fermi surface. Data for temperatures 1.96 K (uppermost trace), 1.34, 1.03, 0.80 to 0.62 K (lowest trace) are shown; for clarity, the data have been offset by 1 Ω (5). (b) High-field experiment, showing higher frequency oscillations due to magnetic breakdown ($T = 480$ mK) (5).

(28). AMROs are measured by rotating a sample in a fixed magnetic field whilst monitoring its resistance; the co-ordinate used to denote the position of AMROs is the polar angle θ between the normal to the sample's layers and the magnetic field. It is also very informative to vary the plane of rotation of the sample in the field; this is described by the azimuthal angle ϕ. The dramatic oscillations in the resistance result from the averaging effect that the semiclassical orbits on the Fermi surface have on the quasiparticle velocity. Both quasione-dimensional and quasitwo-dimensional Fermi-surface sections can give rise to AMROs; in the former case, the AMROs are sharp dips in the resistivity, periodic in $\tan\theta$; in the latter case, one expects *peaks*, also periodic in $\tan\theta$ (3,28). In order to distinguish between these two cases, it is necessary to carry out the experiment at several different ϕ. The ϕ-dependence of the AMROs can be related directly to the shape of a quasitwo-dimensional Fermi-surface section; in the case of a quasione-dimensional sheet, the AMROs yield precise information about the sheet's orientation (3,4,28). Typical data are shown in Fig. 5.

Finally, high-frequency techniques have recently been applied to discover more about the detailed Fermi-surface topology and interactions in charge-transfer salts. In *cyclotron resonance*, photons of frequency ν can be used to excite quasiparticles between Landau levels (see Eq. [2]) (3,10). The fundamental resonance occurs when $\hbar\omega_c = h\nu$; for laboratory fields ($B \sim 1$–20 T) and the typical effective

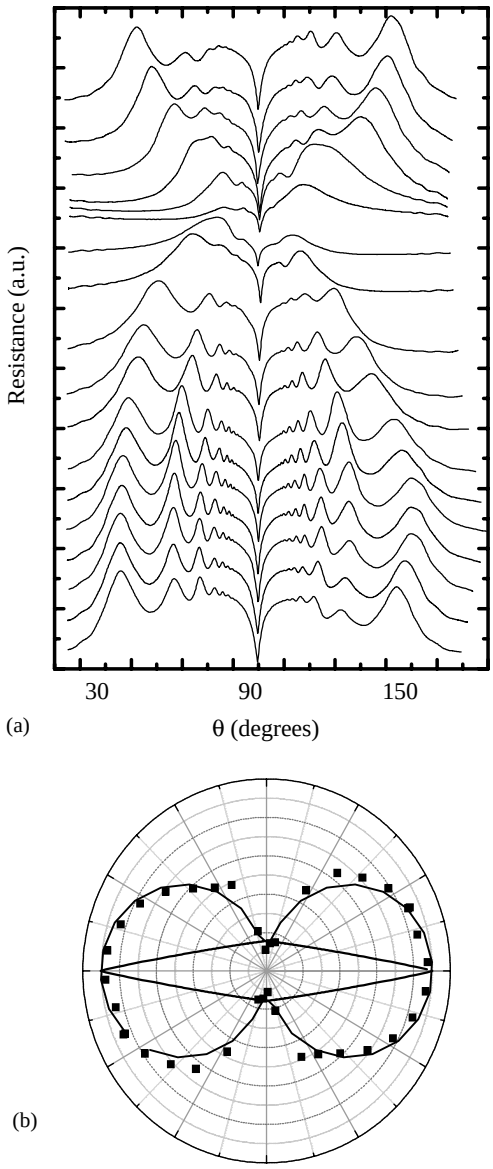

FIG. 5. (a) AMRO data for β-(BEDT-TTF)$_2$SF$_5$CH$_2$CF$_2$SO$_3$ at 10 T and 1.5 K for ϕ-angles $7\pm1^\circ$ (top trace) $17\pm1^\circ$, $27\pm1^\circ$–$177\pm1^\circ$ (bottom trace-adjacent traces spaced by $10\pm1^\circ$). $\phi = 0$ corresponds to rotation in the **a*c*** plane of the crystal to within the accuracy of the infrared orientation used. (b) The ϕ dependence of the $\tan\theta$ periodicity of the AMRO in (a) (points); the "figure of eight" solid curve is a fit. The resulting fitted FS pocket (elongated diamond shape) is shown within. The long axis of the pocket makes an angle of $68\pm4^\circ$ with the **b***-axis (after Ref. (28)).

masses observed in charge-transfer salts (3), this corresponds to photon frequencies in the millimetre-wave range, $\nu \sim 10$–100 GHz. A second GHz technique is a high-frequency variant of AMROs, known as the *Fermi-surface-traversal resonance* (FTR). This technique allows additional information about the topology and corrugations of quasione-dimensional Fermi sheets to be deduced. Cyclotron resonance has been reviewed in Refs. (5,29); descriptions of the FTR are given in Refs. (3,29).

All of these techniques have ensured that (in contrast to the case of the other popular layered systems, such as the "High-T_c" cuprates) the Fermi surfaces of the charge-transfer salts are very well known and very precisely measured. Since many of the energy bands may also be described by *analytical* expressions to a high degree of accuracy, this makes the charge-transfer salts ideal for theoretical modelling (9).

6. UNCONVENTIONAL SUPERCONDUCTIVITY IN CHARGE-TRANSFER SALTS

Superconductivity usually occurs when two electrons or holes of equal and opposite momentum become weakly bound into a "Cooper pair" (30). The binding occurs because the electrons or holes exchange some sort of virtual excitation; in the Bardeen–Cooper–Schrieffer (BCS) explanation of conventional superconductors, this excitation is a phonon, i.e., a vibration of the crystal lattice (30). In conventional superconductors, an energy gap 2Δ then opens up at the energy of the highest occupied electron state (the Fermi energy); this gap separates the superconducting pairs from any normal electrons that may remain (30).

In the organic superconductors, most data strongly suggest that the superconducting energy gap is not uniform, but that there are "nodes", that is regions, or directions, over which the energy gap tends to zero (5). Direct evidence for this has come from scanning-tunnelling microscopy (STM) studies of single crystals at low temperatures (31). Figure 6 shows typical data; it is obvious even from the raw data that the (dI/dV) curves are quite strongly affected by the in-plane tunnelling direction (defined in the figure by the angle ϕ). By contrast, in the case of a conventional superconductor in which the energy gap is uniform, one would expect tunnelling characteristics which were isotropic. Such data have been fitted to a d-wave gap model with some success, yielding maximum values for the energy gap of $2\Delta_0/k_BT_c \approx 6.7$, where T_c is the transition temperature into the superconducting state (31). This is substantially larger than the BCS prediction of $2\Delta_0/k_BT_c \approx 3.5$ (30), again suggesting that the superconductivity in the organics is not the conventional type involving phonons.

Nuclear magnetic resonance (NMR) has also been very important in illustrating the unusual nature of the superconductivity in charge-transfer salts (6). The temperature dependence of the NMR relaxation rates and Knight shifts carried out by three independent groups (32) show behavior reminiscent of the high-T_c cuprates, in which antiferromagnetic fluctuations dominate; a characteristic feature of conventional superconductors, "the Hebel–

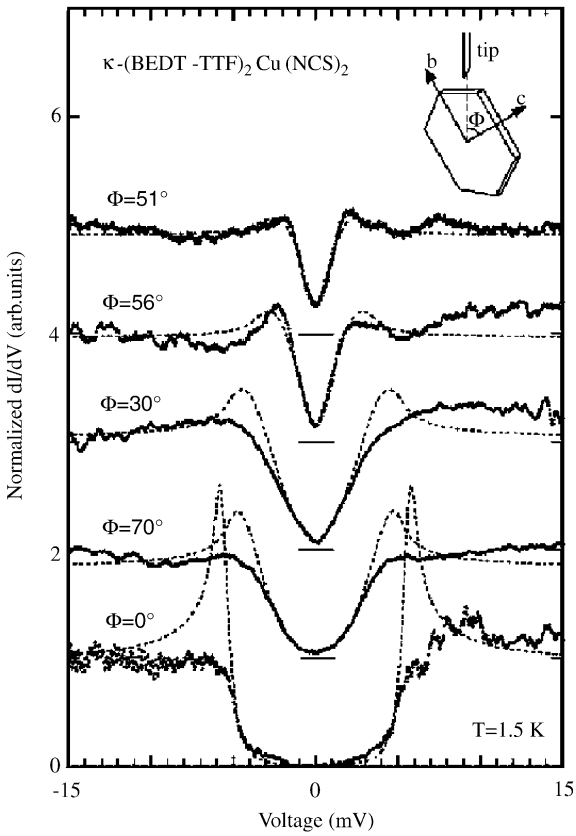

FIG. 6. Tunnelling data on single crystals of the organic superconductor κ-(BEDT-TTF)$_2$Cu(NCS)$_2$ for several different directions of the tunnelling current (see inset). The data (thick lines) are shown as the derivative of the tunnelling current I with respect to the bias voltage V, (dI/dV). The dip in the middle of the data corresponds to the energy gap between the superconducting and normal electron states in κ-(BEDT-TTF)$_2$Cu(NCS)$_2$. If κ-(BEDT-TTF)$_2$Cu(NCS)$_2$ were a conventional BCS superconductor with a roughly uniform energy gap, then one would expect the central dip to be independent of tunnelling direction. Instead, the dip varies strongly, indicating that there are certain directions at which there are *nodes*, i.e., at which the superconducting energy gap disappears. Such data are strong evidence that the superconductivity in organics is unconventional; the dotted line is the expected result from a simple *d*-wave model of superconductivity (31).

Slichter peak'', is also absent. Figure 7 shows a phase diagram deduced from recent NMR and ac susceptibility data, carried out on single crystals of κ-(BEDT-TTF)$_2$Cu(N(CN)$_2$)Cl within a hydrostatic helium gas-pressure cell (6). As has been mentioned above, at low pressures, this salt is an insulator. Below 25 K, the magnetic moments of the conduction holes become ordered into an antiferromagnetic (AF) state; in other words, alternate holes, each localized on a dimer (pair of molecules—see Fig. 1), have opposite spin. As the temperature rises, the magnetic order disappears, and the system is a paramagnetic insulator (PI) (6).

On increasing the pressure, the high-temperature phase of κ-(BEDT-TTF)$_2$Cu(N(CN)$_2$)Cl becomes metallic (M); in other words the holes are free to move about the crystal, conducting electricity. At low temperatures, the increases of pressure result in unconventional superconductivity (U-SC). Over a restricted region (shaded), there is an inhomogeneous phase within which superconductivity coexists with regions of antiferromagnetism (6).

There are several interesting points arising from this phase diagram. First, there is a great similarity between Fig. 7 and the phase diagrams of the high-T_c cuprates and heavy-fermion compounds (3,7). In all of these cases, the superconducting region of the phase diagram is in close proximity to antiferromagnetism, suggesting that antiferromagnetic fluctuations are important in the superconducting mechanism; indeed it is suggested that antiferromagnetic fluctuations, rather than phonons, may well carry the pairing interaction in organics (5). Second, note the absence of a continuous boundary between the metallic and antiferromagnetic phases. This confirms that there is no itinerant antiferromagnetism in κ-phase BEDT-TTF salts; the magnetic order may be understood in terms of interacting hole spins localized on dimers, and is not in any way related to the Cu present in the anions (6).

Further support for this picture of unconventional superconductivity with energy gap nodes in the organics has come from a variety of techniques, including muon-spin relaxation (μSR) (33), penetration–depth measurements (34), and thermal conductivity experiments (35).

Theoretical work on the superconducting state in charge-transfer salts is beginning to acknowledge the one clear advantage that these materials have as a playground for exotic superconductivity; electronic bands which have been measured to great precision, and which can often be represented analytically (8,37). Using this as a starting point, theoretical work has reproduced the node pattern suggested by the tunnelling experiments, and accounted successfully for many of the NMR data (9,36).

7. OPTICAL STUDIES OF CHARGE-TRANSFER SALTS

Charge-transfer salts have been studied extensively using optical methods such as reflectivity and Raman scattering. There are several good motivations for examining the infrared reflectivity; (i) reflectivity can potentially probe low-energy excitations which are characteristic of the bare, undressed, band electrons (5,38); (ii) models (e.g., Ref. (39)) can be used to obtain an indication of phonon-specific electron–phonon interactions (40) from reflectivity data; (iii) the mid-infrared reflectivity of organic molecular metals exhibits a large ''hump'', which has been interpreted as a direct measure of the Coulomb correlation energy (41). Thus, infrared studies potentially enable effects due to the bare bandstructure, the electron–phonon interactions and

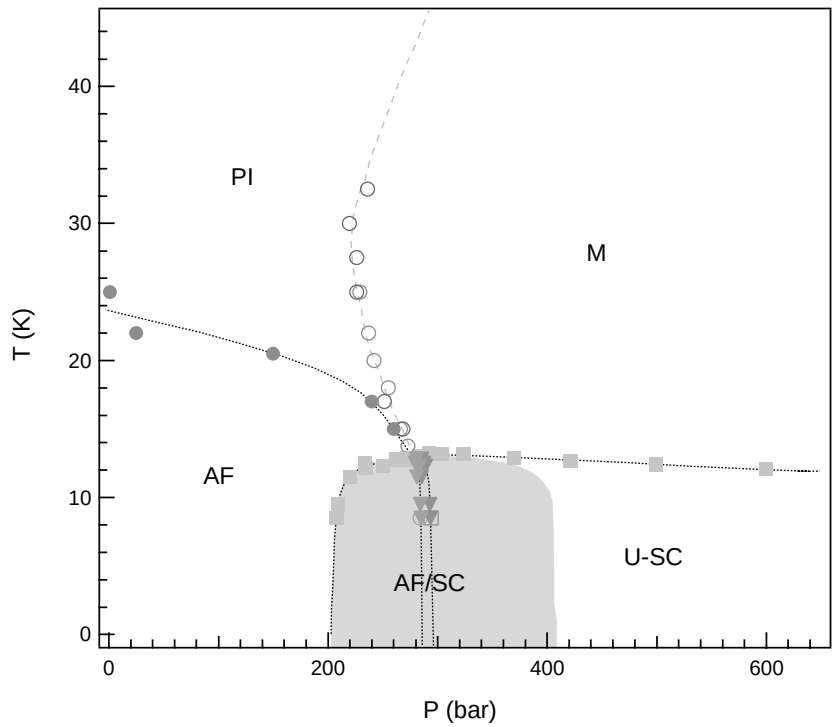

FIG. 7. Temperature versus pressure phase diagram of κ-(BEDT-TTF)$_2$Cu(N(CN)$_2$)Cl deduced using NMR and ac susceptibility measurements. At low pressures, the material is a (Mott) insulator, exhibiting antiferromagnetic (AF) order at low temperatures. As the temperature rises, the magnetic order disappears, and the system is a paramagnetic insulator (PI). On increasing the pressure, the high-temperature phase of κ-(BEDT-TTF)$_2$Cu(N(CN)$_2$)Cl becomes metallic (M); at low temperatures, the increases of pressure result in unconventional superconductivity (U-SC). Over a restricted region (AF/SC, shaded), there is an inhomogeneous phase within which superconductivity coexists with regions of antiferromagnetism (6).

the electron–electron interactions to be distinguished (40,42).

Figures 8 and 9 show typical data, either as raw reflectivity (Fig. 8(a) and 8(b)) or as conductivity derived from the reflectivity (43,44). Note the presence of the broad "hump" around 3000 cm^{-1} mentioned above, the sharp lines due to phonons and the low-frequency conductivity, which increases as the temperature is lowered (Fig. 8(c) and 8(d)) and/or the pressure is raised (Fig. 9). The latter feature is interpreted as a Drude (10) peak (see Refs. (43,44) and references therein), which becomes more prominent as the material's metallic character increases with increasing pressure or decreasing temperature.

The interpretation of reflectivity data from the κ-phase BEDT-TTF salts is still somewhat varied. For example, Wang *et al.* argue quite convincingly that data such as those in Fig. 8 are best understood in terms of polaron absorption (see Ref. (44) and references therein). The broad hump, most prominent at high temperatures, is interpreted as photon-assisted hopping of small polarons (c.f. Ref (41)); the sharp Drude peak that develops at low temperature together with spectral weight in the mid-infrared are attributed to coherent and incoherent bands of large polarons. Thus, Wang *et al.* associate the transition from insulating-like behavior at high temperature to metallic behavior at low temperature seen in many BEDT-TTF salts (2,5) with a crossover from localized small polarons to coherent large polarons (44).

Optical techniques have been extensively applied to superconducting charge-transfer salts and suggest that electron–phonon interactions, antiferromagnetic fluctuations *and* perhaps other types of electron–electron interactions are all important (or at least in some way involved) in the mechanism for superconductivity (5). A particularly elegant experiment has shown the softening (i.e., moving to lower frequencies) of phonon modes at the temperature at which the antiferromagnetic fluctuations which are a precursor of superconductivity start to occur (45). Some representative data are shown in Fig. 10, which shows the normalized frequency of the $\nu_9 A_g$ mode in α-(BEDT-TTF)$_2$I$_3$, β-(BEDT-TTF)$_2$AuI$_2$, κ-(BEDT-TTF)$_2$Cu(N(CN)$_2$)Br and κ-(d8-BEDT-TTF)$_2$Cu(N(CN)$_2$Br as a function of temperature; in the latter material, the eight terminal hydrogens have been replaced with deuterium. For α-(BEDT-TTF)$_2$I$_3$ and β-(BEDT-TTF)$_2$AuI$_2$, the usual hardening (increase in frequency) of the mode occurs

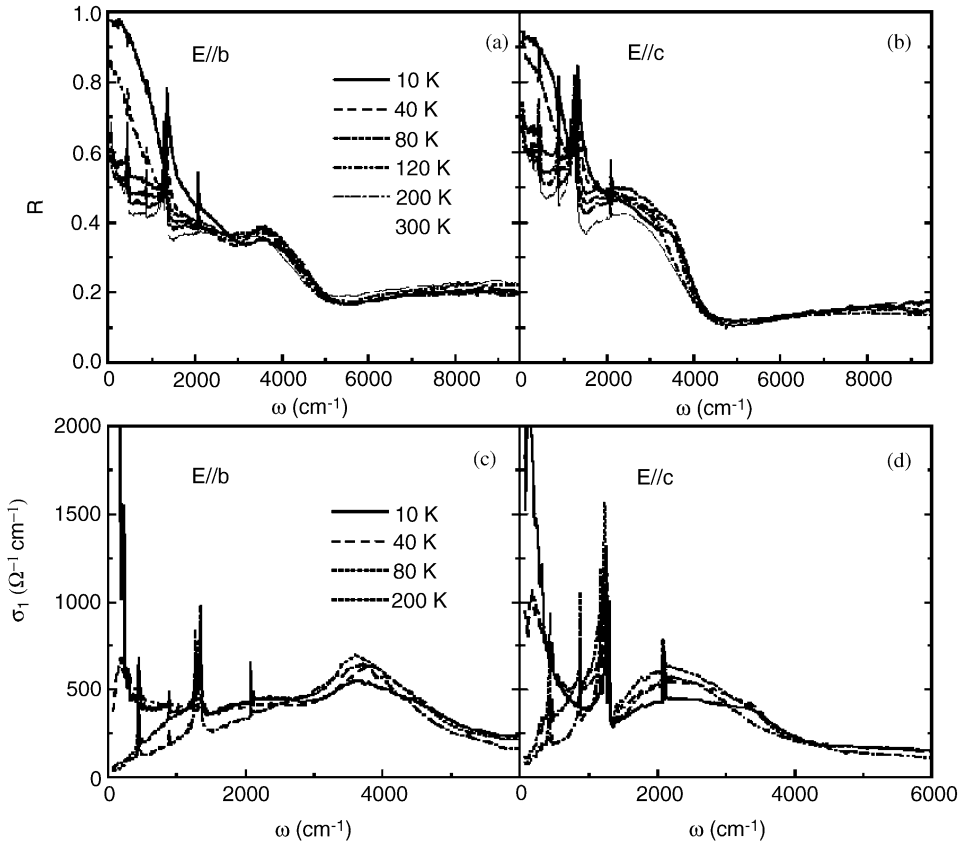

FIG. 8. Reflectivity of κ-(BEDT-TTF)$_2$Cu(NCS)$_2$ as a function of photon energy for infrared polarized parallel **b** (a) and **c** (b) respectively. Data for several temperatures are shown. (c) and (d) show the corresponding frequency-dependent conductivity, $\sigma(\omega)$ (after Ref. (44)). Note the sharp peaks due to phonons and the increase in low-frequency conductivity (i.e., metallic behavior) as the temperature decreases.

as the lattice contracts with decreasing temperature. However, in the case of the two κ-phase salts, softening (reduction in frequency) occurs below the temperature at which antiferromagnetic fluctuations, measured in NMR studies (45), become important (45). Note that α-(BEDT-TTF)$_2$I$_3$ has no antiferromagnetic fluctuations present (45).

8. UNUSUAL MAGNETIC-FIELD-INDUCED GROUNDSTATES

An attraction of charge-transfer salts is the wide range of low-temperature groundstates that they can exhibit; semimetallic, superconducting, semiconducting, magnetic and density-wave states are all possible (2,3). Moreover, it is often possible to tune between these states using pressure and/or high magnetic fields (2,3). In this section, I describe three recent instances of interesting states induced by high magnetic fields.

It is well known that superconductivity is destroyed by the application of a sufficiently high magnetic field (10). However, there have been two recent reports of superconducting states in organic conductors which are *only observed in high magnetic fields*. The first to be observed was the Fulde–Ferrell–Larkin–Ovchinnikov (FFLO) state, an effect which was predicted in the 1960s (46) but only observed experimentally on in 2000 (47).

As has already been mentioned, superconductivity usually occurs when two electrons or holes of equal and opposite momentum become weakly bound into a "Cooper pair" (10). In an energy band picture, the pairing results from electrons or holes at the highest occupied energy level (the Fermi energy) interacting with their counterparts on the opposite side of the band (see Fig. 11). At large magnetic fields, the band is split into two; this occurs because each electron or hole can have spin up or spin down, and the Zeeman energy associated with the interaction between the electron or hole's spin and the magnetic field means that the two spin states no longer have the same energy. In the FFLO state, an electron or hole on one side of the "spin up" band pairs with a

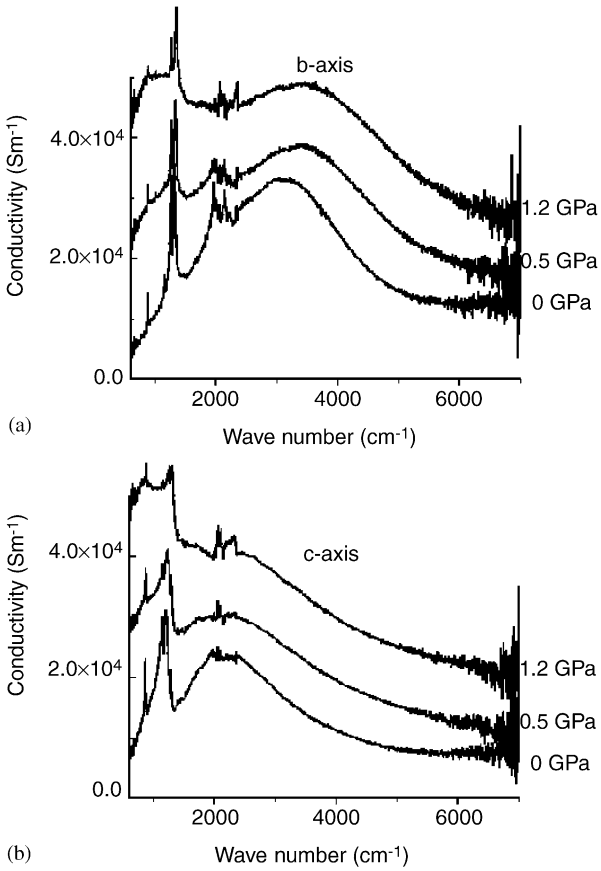

FIG. 9. Room temperature frequency-dependent conductivity $\sigma(\omega)$ of for κ-(BEDT-TTF)$_2$Cu(NCS)$_2$ infrared polarized parallel to **b** (top) and **c** (bottom) for pressures 0, 0.5 and 1.2 Gpa (after Ref. (43)). Note the increase in low-frequency conductivity as the pressure increases.

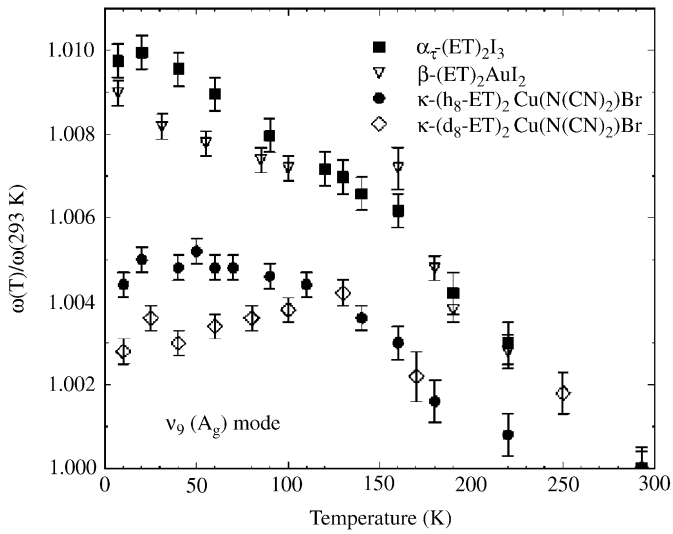

FIG. 10. Normalized frequency of the ν_9 (A_g) mode in α-(BEDT-TTF)$_2$I$_3$, β-(BEDT-TTF)$_2$AuI$_2$, κ-(BEDT-TTF)$_2$Cu(N(CN)$_2$)Br and κ-(d8-BEDT-TTF)$_2$Cu(N(CN)$_2$)Br as a function of temperature; in the latter material, the eight terminal hydrogens have been replaced with deuterium. For α-(BEDT-TTF)$_2$I$_3$ and β-(BEDT-TTF)$_2$AuI$_2$, the usual hardening (increase in frequency) of the mode occurs as the lattice contracts with decreasing temperature. However, in the case of the two κ-phase salts, softening (reduction in frequency) occurs below the temperature at which antiferromagnetic fluctuations become important (after Ref. (45)).

companion on the opposite side of the "spin-down" band (46). As its members no longer have equal and opposite momentum, the resulting "Cooper pair" now has a finite momentum (Fig. 11).

Superconductivity is usually suppressed by a field via orbital interactions; orbital interactions involve the energy associated with the well-known tendency of charged particles (electrons or holes) to perform closed orbits in a plane perpendicular to a magnetic field. A quasitwo-dimensional charge-transfer salt can get around this problem *if the magnetic field is applied exactly in the plane of the layers*. In such a configuration, only a very tiny number of closed orbits can occur in the plane perpendicular to the applied field (12,47). Hence, the orbital interactions which would otherwise overwhelm the superconductivity are suppressed (48).

The FFLO state is therefore observed only when the magnetic field is very close to the interlayer direction, and Fig. 11 shows a typical phase diagram for the organic superconductor κ-(BEDT-TTF)$_2$Cu(NCS)$_2$ in such a field (47). Notice that the FFLO state is more stable in high fields than more "conventional" superconductivity; as a result it occupies the top left-hand corner of the phase diagram, resulting in a considerable enhancement of the upper critical field (48). By contrast, the orbitally limited upper critical fields are a factor 5–10 lower when the field is applied perpendicular to the layers (5).

The second example is λ-(BETS)$_2$FeCl$_4$, which shows a transition to what appears to be a superconducting state in an accurately in-plane magnetic field (14,49) (Fig. 12). In this salt, the Fe^{3+} ions within the $FeCl_4$ anion molecules order antiferromagnetically at low temperatures and low magnetic fields (see Ref. (49) and references therein). As is the case in most antiferromagnetic materials, the magnetic order causes λ-(BETS)$_2$FeCl$_4$ to become an insulator. On raising the magnetic field (applied exactly within the planes), the magnetic moments of the Fe^{3+} ions tilt (i.e., become "canted"), and then the long-range magnetic order is destroyed, leaving a paramagnetic metal (49). Further increases in field induce the superconducting state at about 16 T (49).

Field-induced superconductivity in magnetic materials is usually discussed in terms of the Jaccarino–Peter compensation (JPC) effect, in which the applied field "compensates" the internal magnetic field provided by the magnetic ions (in the case of λ-(BETS)$_2$FeCl$_4$, the Fe^{3+} ions). The

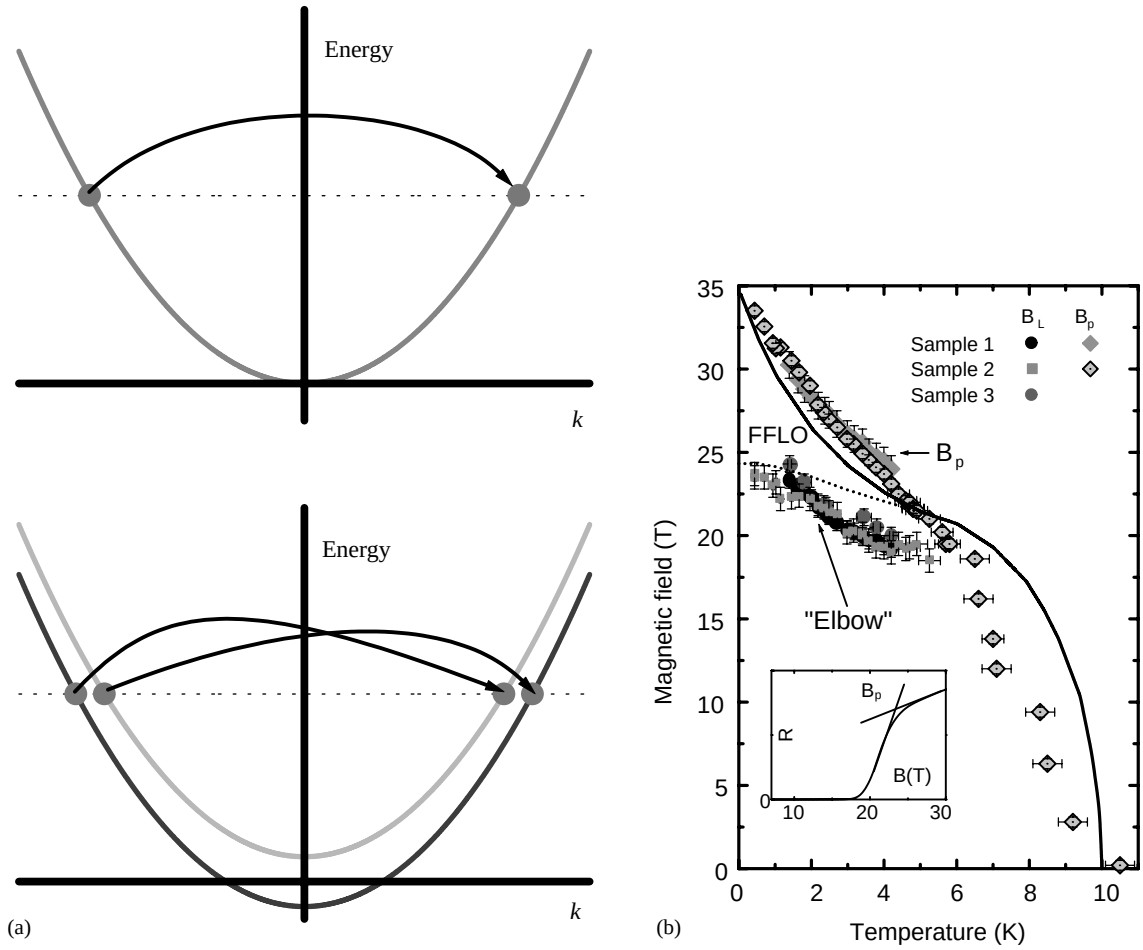

FIG. 11. Some of the high-field states observed in organic superconductors. Left-hand side; top, a cartoon of conventional superconductivity in a simple electronic band; the band is plotted as energy versus wavevector k. Electrons (dots) close to the highest occupied energy level (the Fermi energy—dotted line) interact to form a Cooper pair. The interaction (arrow) is only strong for electrons of equal and opposite momentum, that is, for electrons with equal and opposite k. In the lower cartoon, a large magnetic field has split the electronic band into two (spin up and spin down) via the Zeeman splitting. The FFLO state occurs when interactions (arrows) pair up electrons (dots) from one side of the spin-up band with those from the opposite side of the spin-down band and vice versa (46). As the electrons no longer have equal and opposite k (momentum), this results in "Cooper pairs" with finite momentum. Right-hand side: experimental observation of the FFLO state in κ-(BEDT-TTF)$_2$Cu(NCS)$_2$ employing magnetic fields applied exactly within the layers (47); the phase boundary between the FFLO and ordinary superconductivity (shaded dots and squares) is observed as an "elbow" at field B_L in a high-frequency measurement of the magnetic susceptibility. The shaded diamonds stretching from (0K, 35T) to around (10K, 0T) correspond to a simultaneous resistive measurement of the upper critical field (inset); note that the presence of the FFLO leads to a considerably enhanced upper critical field. The curves are theoretical phase boundaries (48).

JPC effect was predicted in the early 1960s (50), and observed almost 20 years ago in $Eu_xSn_{1x}Mo_6S_8$ (51).

Therefore, the situation in λ-(BETS)$_2$FeCl$_4$ seems to be as follows. The applied magnetic field compensates the internal field provided by the Fe^{3+} ions, so that superconductivity (which would otherwise be suppressed by the magnetism) can occur at fields above 16–20 T (14,49). Above I described how a quasitwo-dimensional superconductor can attain high upper critical fields *if the magnetic field is applied exactly in the plane of the layers*. In such a configuration, only a very small number of closed orbits can occur on the Fermi surface. Hence, the orbital interactions which would otherwise overwhelm the superconductivity are suppressed (5). The magnetic field can then only destroy the superconductivity via the Zeeman effect, leading to an upper critical field determined by the Pauli limit or a more exotic mechanism such as the FFLO. It is notable that the field-induced superconductivity in λ-(BETS)$_2$FeCl$_4$ *only* occurs when the magnetic field is exactly within the layers.

Brooks has pointed out that the behavior of λ-(BETS)$_2$FeCl$_4$ in an in-plane magnetic field looks almost

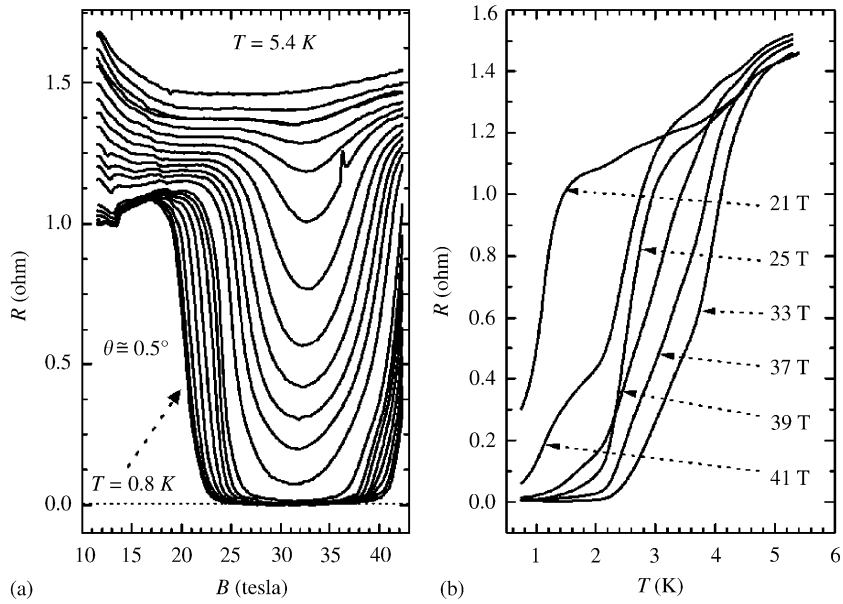

FIG. 12. Resistance of a crystal of λ-$(BETS)_2FeCl_4$ (a) as a function of magnetic field for temperatures between 800 mk and 5.4 K and (b) as a function of temperature for various magnetic fields (after Ref. (14)). The magnetic field is applied within the quasitwo-dimensional planes of the crystal. Note the strong minimum in the resistance, suggestive of superconductivity.

exactly like that of its isostructural sister λ-$(BETS)_2GaCl_4$, except that the characteristic in-plane fields in the former material are "offset" by 33 T (52). The 33 T offset may be identified with the field needed to compensate the effective field due to the Fe^{3+} ions; once this is done, λ-$(BETS)_2FeCl_4$ and λ-$(BETS)_2GaCl_4$ behave almost identically.

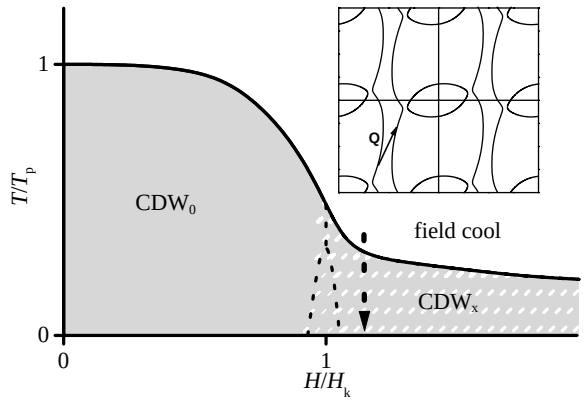

FIG. 13. The H–T phase diagram of α–K and α–Rb. The corresponding zero-field transition temperatures T_p for α–K and α–Rb are 8 and 10 K, respectively, while the characteristic median fields $\mu_0 H_k$ at which the CDW_0 to CDW_x transition occurs are 23 and 32 T, respectively. $\mu_0 H_k$ is hysteretic between rising and falling fields at low temperatures, depicted by the splitting of the dotted phase boundary line. The thick, dashed vertical arrow indicates the path taken within the phase diagram on performing a field cool. The inset shows the in-plane Fermi surface in the repeated Brillouin zone representation. The "CDW nesting vector" **Q** approximately maps the two opposing sections of the open Fermi surface onto each other (53,54).

The final example of an exotic field-induced phase occurs in the salt α-$(BEDT\text{-}TTF)_2KHg(SCN)_4$ (53). Whilst it exhibits many of the features associated with superconductivity, including a resistive transition and persistent currents, it is probably not a superconductor at all, but something rather more exotic.

At low magnetic fields, the material in question, α-$(BEDT\text{-}TTF)_2KHg(SCN)_4$, is not a superconductor, but a charge-density-wave system (53) (Fig. 13). In a charge-density wave, the conduction electrons or holes arrange themselves periodically; thus, the charge density is spatially modulated in a wave-like manner (55). In virtually all instances, this leads to an electrical insulator, because an energy gap opens up at the Fermi energy and the charge-density wave becomes pinned to any defects or dirt that happens to be present in the crystal (55).

However, on increasing the magnetic field, the CDW_0 charge-density wave phase in α-$(BEDT\text{-}TTF)_2KHg(SCN)_4$ undergoes a transition into another phase, called the CDW_x phase. Although the CDW_x phase appears to have some of the properties of a charge-density wave, it exhibits some surprising tendencies; the resistivity drops very sharply as the temperature is lowered in a manner exactly

like that in inhomogeneous superconductors (53). Moreover, the samples exhibit what appear to be long-duration persistent currents, normally a hallmark of superconductivity (53,56).

That some form of conventional superconductivity might emerge in a charge density-wave system at high magnetic fields is highly unlikely, and explanations of the experimental observations in α-(BEDT-TTF)$_2$KHg(SCN)$_4$ may involve the dissipationless sliding of the density wave of the CDW$_x$ phase as it tries to minimize its free energy whilst the magnetic field changes (56,57).

9. SUMMARY

I hope that I have illustrated some of the reasons why physicists are increasingly fond of charge-transfer salts. This enthusiasm is likely to continue for some time, as the charge-transfer salts offer great versatility as a plaything for studying the formation of bandstructure. Using the known self-organizational properties of small organic molecules, one can really indulge in "molecular architecture", in which the structure of a charge-transfer salt is adjusted to optimize a desired property (1). The most imaginative essays in this field involve the use of molecules that introduce a further property which modifies the electronic behavior, such as chirality or the presence of magnetic ions (58).

There are also many reasons for continuing to study charge-transfer salts at high magnetic fields. A particular goal is the ultraquantum limit, in which only one quantized Landau level is occupied; phenomena such as yet more varieties of field-induced superconductivity have been predicted to occur once such a condition is attained (3). Furthermore, there are many open questions about the role of chiral Fermi liquids in such fields (3). Another area of considerable interest is the observation of magnetic breakdown. At fields above 50 T, the magnetic energy of the holes in the organic superconductors is starting to become a substantial fraction of their total energy, and one gradually starts to approach the famous Hofstadter "butterfly" limit (3). Watch this space!

ACKNOWLEDGMENTS

Work on organic conductors at Oxford is supported by EPSRC (UK). I should like to thank Albert Migliori, Paul Goddard, Arzhang Ardavan, Chuck Mielke, Anne-Katrin Klehe, Francis Pratt, Stan Tozer, Neil Harrison, Bill Hayes, Francis Pratt, Jim Brooks, Joerg Schmalian, Luis Balicas, Phil Anderson and Steve Blundell for useful discussions and encouragement.

REFERENCES

1. T. Mori, *Bull. Chem. Soc. Jpn.* **71,** 2509 (1998); T. Mori, H. Mori, and S. Tanaka, *Bull. Chem. Soc. Jpn.* **72,** 179 (1999); T. Mori, *Bull. Chem. Soc. Jpn.* **72,** 2011 (1999).
2. T. Ishiguo, K. Yamaji, and G. Saito, "Organic Superconductors." Springer-Verlag, Berlin, 1998.
3. J. Singleton, *Rep. Progr. Phys.* **63,** 1111 (2000).
4. J. Wosnitza, "Fermi Surfaces of Low-Dimensional Organic Metals and Superconductors." Springer-Verlag, Berlin, 1996; J. Wosnitza, *Curr. Op. Solid State Mater. Sci.* **5,** 131 (2001).
5. J. Singleton and C. H. Mielke, *Contemp. Phys.* **43,** 63 (2002).
6. S. Lefebvre, P. Wzietek, S. Brown, C. Bourbonnais, D. Jerome, C. Meziere, M. Fourmigue, and P. Batail, *Phys. Rev. Lett.* **85,** 5420 (2000).
7. R. McKenzie, *Comment. Cond. Mat. Phys.* **18,** 309 (1998); H. Kanoda, *Physica C* **282,** 299 (1997); *Hyperfine Interactions* **104,** 235 (1997).
8. J. Schmalian, *Phys. Rev. Lett.* **81,** 4232 (1998).
9. K. Kuroki, T. Kimura, R. Arita, Y. Tanaka, and Y. Matsuda, preprint cond-mat 0108506 (2001).
10. N. W. Ashcroft and N. D. Mermin, "*Solid State Physics.*" Saunders, London, 1976; J. Singleton, "Band Theory and Electronic Properties of Materials." Oxford University Press, Oxford, 2001.
11. H. Urayama, H. Yamochi, G. Saito, S. Sato, A. Kawamoto, J. Tanaka, H. Mori, Y, Maruyama, and H. Inokuchi, *Chem. Lett.* **1988,** 463 (1988).
12. John Singleton, P. A. Goddard, A. Ardavan, N. Harrison, S. J. Blundell, J. A. Schlueter, and A. M. Kini, *Phys. Rev. Lett.* **88,** 037001 (2002).
13. Charles Mielke, John Singleton, Moon-Sun Nam, Neil Harrison, C. C. Agosta, B. Fravel, and L. K. Montgomery, *J. Phys.: Condens. Matter* **13,** 8325 (2001).
14. L. Balicas, J. S. Brooks, K. Storr, S. Uji, M. Tokumoto, H. Tanaka, H. Kobayashi, A. Kobayashi, V. Barzykin, and L. P. Gor'kov, *Phys. Rev. Lett.* **87,** 067002 (2001).
15. E. Laukhina, J. U. A. Khomenko, S. Pesotskii, V. Tchachev, L. Atovmyan, E. Yagubski, C. Robira, J. Veciana, J. Vidal-Gancedo, and V. Laukhin, *J. Phys. I.* (France) **7,** 1665 (1997).
16. R. McDonald, H. Brom, E. Laukhina, and J. Singleton, *Synth. Met.* **121,** 867 (2001).
17. N. Toyota, E. W. Fenton, T. Sasaki, and M. Tachiki, *Solid State Commun.* **72,** 859 (1989).
18. E. Demiralp and W. A. Goddard III, *Phys. Rev. B* **56,** 11907 (1997).
19. M. V. Kartsovnik, V. N. Laukhin, S. I. Pesotskii, I. F. Schegolev, and V. M. Yakovenko, *J. Phys. I* (Paris) **2,** 89 (1990).
20. A. B. Pippard, *Proc. Roy. Soc. A* **270,** 1 (1962); *Proc. Roy. Soc. A* **287,** 165 (1965).
21. N. Harrison, J. Caulfield, J. Singleton, P. H. P. Reinders, F. Herlach, W. Hayes, M. Kurmoo, and P. Day, *J. Phys.: Condens. Matter* **8,** 5415 (1996).
22. J.-Y. Fortin and T. Ziman, *Phys. Rev. Lett.* **80,** 3117 (1998); J. -Y. Fortin and T. Ziman, *Phys. Rev. Lett.* **82,** 4148 (1999).
23. A. C. Hewson, "The Kondo Problem to Heavy Fermions." Cambridge University Press, Cambridge, 1993; E. G. Haanappel, *Physica B* **246–247,** 78 (1998) and references therein; A. Wasserman and M. Springford, *Adv. Phys.* **45,** 471 (1996).
24. D. Shoenberg, "Magnetic Oscillations in Metals." Cambridge University Press, Cambridge, 1984.
25. K. Oshima, T. Mori, H. Inokuchi, H. Urayama, H. Yamochi, and G. Saito, *Phys. Rev. B* **38,** 938 (1988).
26. F. L. Pratt, A. J. Fisher, W. Hayes, J. Singleton, S. J. R. M. Spermon, M. Kurmoo, and P. Day, *Phys. Rev. Lett.* **61,** 2721 (1988).

27. W. Kang, G. Montambaux, J. R. Cooper, D. Jerome, P. Batail, and C. Lenoir, *Phys. Rev. Lett.* **62,** 2559 (1989).
28. M. S. Nam, S. J. Blundell. A. Ardavan, J. A. Symington, and J. Singleton, *J. Phys: Condens. Matter* **13,** 2271 (2001); S. J. Blundell and J. Singleton, *J. Phys. I* **6,** 1837 (1996).
29. J. M. Schrama, J. Singleton, R. S. Edwards, A. Ardavan, E. Rzepniewski, R. Harris, P. Goy, M. Gross, J. Schlueter, M. Kurmoo, and P. Day, *J. Phys.: Condens. Matter* **13,** 2235 (2001)
30. C. P. Poole, H. A. Farach, and R. J. Creswick, "Superconductivity." Academic Press, San Diego, 1995.
31. T. Arai, K. Ichimura, K. Nomura, S. Takasaki, J. Yamada, S. Nakatsuji, and H. Anzai, *Phys. Rev. B* **63,** 104518 (2001).
32. S. M. de Soto, C. P. Slichter, A. M. Kini, H. H. Wang, U. Geiser, and J. M. Williams, *Phys. Rev. B* **52,** 10364 (1995); S. M. de Soto, C. P. Slichter, A. M. Kini, H. H. Wang, U. Geiser, and J. M. Williams, *Phys. Rev. B* **54,** 16101 (1996); H. Mayaffre, P. Wzietek, D. Jérome, C. Lenoir, and P. Batail, *Phys. Rev. Lett.* **75,** 4122 (1995); K. Kanoda, K. Miyagawa, A. Kawamoto, and Y. Nakazawa, *Phys. Rev. B* **54,** 76 (1996).
33. F. L. Pratt, S. L. Lee, C. M. Aegerter, C. Ager, S. H. Lloyd, S. J. Blundell, F. Y. Ogrin, E. M. Forgan, H. Keller, W. Hayes, T. Sasaki, N. Toyota, and S. Endo, *Synth. Met.* **120,** 1015 (2001).
34. A. Carrington, I. J. Bonalde, R. Prozorov, R. W. Gianetta, A. M. Kini, J. Schlueter, H. H. Wang, U. Geiser, and J. M. Williams, *Phys. Rev. Lett.* **83,** 4172 (1999).
35. K. Izawa, H. Yamaguchi, T. Sasaki, and Y. Matsuda, *Phys. Rev. Lett.* **88,** 027002 (2002).
36. S. Charf fi-Kaddour, A. Ben Ali, M. Heritier, and R. Bennaceur, *J. Supercond.* **14,** 317 (2001); R. Louati, S. Charfi-Kaddour, A. Ben Ali, R. Bennaceur, and M. Heritier, *Phys. Rev. B* **62,** 5957 (2000); Won-Min Lee, *Solid State Commun.* **106,** 601 (1998).
37. A. Girlando, M. Massino, A. Brilliante, R. G. Della Valle, and E. Venuti, preprint cond-mat 0202141 (February 2002).
38. K. F. Quader. K. S. Bedell, and G. E. Brown, *Phys. Rev. B* **36,** 156 (1987); A. J. Leggett, *Ann. Phys.* **46,** 76 (1968).
39. M. J. Rice, *Phys. Rev. Lett.* **37,** 36 (1976).
40. O. O. Drozdova *et al.*, *Synth. Met.* **64,** 17 (1994).
41. S. Mazumdar and S. N. Dixit, *Phys. Rev. B* **34,** 3683 (1986).
42. M. J. Rozenberg *et al.*, *Phys. Rev. B* **54,** 8452 (1996).
43. A.-K. Klehe, R. D. McDonald, A. F. Goncharov, V. V. Struzhkin, H.-K. Mao, R. J. Hemley, T. Sasaki, W. Hayes, and J. Singleton, *J. Phys.: Condens. Matter* **12,** L247 (2000).
44. N. L. Wang, B. P. Clayman, H. Mori, and S. Tanaka, *J. Phys.: Condens. Matter* **12,** 2867 (2000).
45. Y. Lin, J. E. Eldridge, J. Schlueter, H. H. Wang, and A. M. Kini, *Phys. Rev. B* **64,** 024506 (2001).
46. P. Fulde and R. A. Ferrell, *Phys. Rev.* **135,** A550 (1964); A. I. Larkin and Yu. N. Ovchinnikov, *Zh. Eksp. Teor. Fiz.* **47,** 1136 (1964); A. I. Larkin and Yu. N. Ovchinnikov, *Sov. Phys. JETP* **20,** 762 (1965).
47. J. Singleton, J. A. Symington, M. S. Nam, A. Ardavan, M. Kurmoo, and P. Day, *J. Phys.: Condens. Matter* **12,** L641 (2000).
48. H. Shimahara, *Phys. Rev. B* **50,** 12760 (1994).
49. S. Uji *et al.*, *Nature* **410,** 908 (2001).
50. V. Jaccarino and M. Peter, *Phys. Rev. Lett.* **9,** 290 (1962).
51. H. W. Meul *et al.*, *Phys. Rev. Lett.* **53,** 497 (1984).
52. J. S. Brooks *et al.*, *Synth. Met.*, in press.
53. N. Harrison, C. H. Mielke, J. Singleton, J. S. Brooks, and M. Tokumoto, *J. Phys.: Condens. Matter* **13,** L389 (2001).
54. N. Harrison, E. Rzepniewski, J. Singleton, P. J. Gee, M. M. Honold, P. Day, and M. Kurmoo, *J. Phys.: Condens. Matter* **11,** 7227 (1999).
55. G. Grüner, "Density Waves in Solids (Frontiers in Physics, Vol. 89.)." Addison-Wesley, Reading, MA, 1994.
56. A. Ardavan, N. Harrison, P. Goddard *et al.*, preprint, Science, submitted.
57. N. Harrison, preprint cond-mat 01110278, *Phys. Rev. Lett.*, submitted.
58. P. Day, *Phil. Trans. R. Soc. Lond. A* (1999), Vol. 357, p. 3163.